# Multiuser Receivers That are Robust to Delay Mismatch

Wei Zha, *Student Member, IEEE*, and Steven D. Blostein, *Senior Member, IEEE*

***Abstract*—We investigate a new robust multiuser signal detector for asynchronous code-division multiple-access uplink channels under delay mismatch. We first formulate a robust decorrelating detector by dividing each user into two virtual users with rectangular chip pulse shapes. To increase the system capacity, a multistage version of the robust decorrelating detector is derived, which can achieve capacity of up to $M/(M+1)$ of the spreading factor, where $M$ is the observation block length. We further propose a robust successive interference cancellation (SIC) implementation. The proposed robust SIC detector adds only a residual error estimation procedure onto the standard SIC detector, so its computational complexity is of the same order of that of the SIC. Performance is investigated via analysis and simulation. Computer simulation results showed that our proposed robust SIC detector outperforms the conventional decorrelating detector when delay estimation error is present, and its performance is close to that of the decorrelating detector with perfect time-delay information. Finally, we generalize the robust SIC detector to the case of nonrectangular chip pulse shapes.**

***Index Terms*—Code-division multiple access (CDMA), delay mismatch, multiuser detection, pulse shaping, robust detection.**

## I. Introduction

A VARIETY of low-complexity multiuser detectors have been proposed in the past decade, including the decorrelating detector [1], the minimum mean-square error (MMSE) detector [2], and the multistage successive interference cancellation (SIC) [3] and parallel interference cancellation (PIC) detector [4]. However, these multiuser detectors all need perfect time-delay information for all the users at the basestation receiver.

In a practical code-division multiple-access (CDMA) communication system, time delays have to be estimated. Existing delay estimation methods include the sliding correlator [6], subspace-based algorithms [7], [8], single-user maximum-likelihood [9], and the large sample maximum-likelihood (LSML) algorithm [10]. For an observation length of 100 symbols, current sliding correlator delay estimation methods [6] can achieve a delay estimation error within 0.2 $T_c$, and the subspace-based MUSIC algorithm can achieve 0.03 $T_c$, where $T_c$ is the chip duration [7].

The effect of imperfect time-delay estimation, i.e., delay mismatch, on the performance of multiuser detectors has been investigated in [11]–[15]. It is shown that these multiuser detectors are sensitive to delay mismatch: bit error rate (BER) performance degrades greatly even with relatively small delay estimation errors under severe near–far scenarios, i.e., 20 dB.

Modified multiuser detectors have, thus, been proposed to mitigate the effects of imperfect time delay. The decorrelating detector [16] and delay-independent decorrelating detector [17] for the quasi-synchronous CDMA (QS-CDMA) channel are based on a deterministic delay error model for a rectangular chip pulse shape. The chip-asynchronous user signal is modeled as the sum of signals from two equivalent chip-synchronous virtual users. The multiple-access interference (MAI) is completely rejected when the true delay and estimated delay are in the same chip interval. However, because they double the number of pseudonoise (PN) codes used, the noise enhancement problem of the decorrelating detector is more severe, and their capacity will not exceed 50% of the spreading factor [17].

The QS-CDMA MMSE detector [16], the improved MMSE (IMMSE) multiuser detector for asynchronous CDMA [26], and two robustified detectors [18] are based on stochastic delay error modeling. The detectors [16] and [26] achieve robustness by averaging over all possible delay errors, assuming zero-mean Gaussian [26] or uniform delay error distribution [16], respectively. In [18], the linear transformation matrix of the MMSE and decorrelating detector is modified. Although the stochastic approach improves the average BER for a large delay error distribution, the residual MAI caused by timing error is not completely eliminated and is, therefore, not near–far resistant.

We consider multiuser detection for the asynchronous CDMA uplink under delay mismatch using a similar approach as in [16] and [17], and chip-matched sampling and filtering. We assume that the delays of all users are estimated to within the same chip interval of the true delay. Our proposed robust multiuser detector is insensitive to time-delay estimation errors, with a capacity close to 100% of the spreading factor, and performs well for bandlimited chip waveforms.

Without loss of generality, we consider a single-path CDMA uplink channel, assuming $K$ active users. We note that an $L$-path, $K$-user channel can be modeled as a single-path system with $K \times L$ users.

For rectangular chip pulses, the equivalent discrete-time user signal can be expressed as the sum of signals from two equivalent virtual users. We divide the two *virtual* users into an *estimated virtual user* with signature waveform at the estimated

Paper approved by R. Kohno, the Editor for Spread Spectrum Theory and Applications of the IEEE Communications Society. Manuscript received October 15, 2000; revised December 15, 2001. This work was supported by the Canadian Institute for Telecommunications Research under the NCE program of the Government of Canada. This paper was presented in part at the IEEE International Conference on Acoustics, Speech, and Signal Processing (ICASSP), Salt Lake City, UT, May 2001.

The authors are with the Department of Electrical and Computer Engineering, Queen's University, Kingston, ON K7L 3N6, Canada (e-mail: wzha@ee.queensu.ca; sdb@ece.queensu.ca).

Digital Object Identifier 10.1109/TCOMM.2002.806548

delay, and one *error virtual user* with signature waveform as the error vector corresponding to the difference between the true delay and estimated delay. Thus, we view a signal from one propagation path as signals arriving from two virtual paths. Since the delay error will only affect the amplitude of those two virtual users' signals, and since it is well known that the decorrelating detector does not require user amplitude information, it is possible to design a robust decorrelating detector for those $2K$ virtual users and eliminate the MAI [17].

To increase capacity beyond 50% of the spreading factor, we use a block of $M$ symbols, and apply the new robust decorrelating detector on a block in a multistage fashion. In each stage, $M$ separate error vectors are combined into an $M$-symbol length error vector using tentative data bit decisions from the previous stage. The result is an equivalent $(M+1)K/M$-user CDMA system, and the system capacity is increased to $M/(M+1)$ of the spreading factor.

Since the multistage decorrelating detector is extremely complex to compute, we propose a robust SIC detector. At each SIC iteration, the delay mismatch-introduced interference is estimated and cancelled using decision feedback from the tentative data bits.

This robust SIC is then generalized to bandlimited chip pulse shapes. Unlike [16] and [26], the robust SIC detector does not require an assumed delay error distribution.

This paper is organized as follows. In Section II, the system models are described. Section III proposes the robust SIC multiuser detector under delay mismatch, and is analyzed in Section IV. Section V generalizes the new detector to bandlimited chip pulse shapes, while Section VI provides simulation results. The symbols $(\cdot)^T$, $(\cdot)^*$, and $(\cdot)^H$ denote transpose, conjugate, and conjugate transpose operations, respectively. $I_M$ denotes an $M \times M$ identity matrix.

## II. System Model

We consider the basestation uplink receiver that has knowledge of the spreading codes of all users. It is assumed that the delays of all users are estimated to within one chip interval of the true delays. For clarity and brevity, we consider a single-path channel. However, the method can be extended to the case of multipath channels in a straightforward manner.

Using a similar system model to [1], the received signals are assumed to be carrier phase-synchronized and coherently received, so the equivalent baseband signal is real

$$r(t) = \sum_i \sum_{k=1}^{K} b_k(i) a_k(i) \tilde{s}_k(t - iT - \tau_k) + n(t) \qquad (1)$$

where $a_k(i) \in \mathcal{R}$ and $b_k(i) \in \{+1, -1\}$ are the $k$th user's received signal amplitude and data bit for the $i$th time interval, respectively, $\tau_k \in [0, T)$ is the $k$th user's propagation delay, $T$ is the bit duration, $K$ is the total number of users, and $n(t)$ is white Gaussian noise. We note that carrier phase-synchronized MAI is a worst-case scenario.

We consider only rectangular chip pulse shapes. The more general case is considered in Section V. In (1), the normalized signature waveform of user $k$, $\tilde{s}_k(t)$, is

$$\tilde{s}_k(t) = \sum_{j=0}^{N-1} c_k(j) h(t - jT_c) \qquad (2)$$

where $N = T/T_c$ is the spreading factor, $\{c_k(j)\}_{j=0}^{N-1}$ is the spreading code, $T_c$ is the chip duration, and $h(t)$ is a rectangular pulse with duration $[0, T_c)$.

The decorrelating detector for asynchronous CDMA channels in [1] is based on an infinite-length bit sequence. Near–far resistance is destroyed, however, when applied to a finite-length observation window, which is known as the edge effect [5]. To focus on the effect of timing errors, we eliminate edge effects by using an isolation bit insertion (IBI) receiver [20], by inserting a blank bit interval every $M$ bit intervals. We want to recover $M$ transmitted data bits of each user, and select the received signal of $(M+1)T$ length for demodulation.

Assuming the channel changes relatively slowly compared to $(M+1)T$, we model the received signal power as constant for this interval, i.e., $a_k(i) = a_k$ for $i = 1, \ldots, M$.

After chip-matched filtering and chip-rate sampling, in vector form we obtain

$$\mathbf{r} = \sum_{i=1}^{M} \sum_{k=1}^{K} b_k(i) a_k \mathbf{d}_k(i) + \mathbf{n} \qquad (3)$$

where

$$\mathbf{r} = [\mathbf{r}^T(1)\ \mathbf{r}^T(2)\ \ldots\ \mathbf{r}^T(M+1)]^T \in \mathcal{R}^{(M+1)N} \qquad (4)$$

$$\mathbf{n} = [\mathbf{n}^T(1)\ \mathbf{n}^T(2)\ \ldots\ \mathbf{n}^T(M+1)]^T \in \mathcal{R}^{(M+1)N}. \qquad (5)$$

The element $\mathbf{r}(m)$ in (4) for the $m$th observation interval is a vector

$$\mathbf{r}(m) = [r(mN+1)\ r(mN+2)\ \ldots\ r(mN+N)]^T \in \mathcal{R}^N. \qquad (6)$$

The noise vector $\mathbf{n}$ is a zero-mean Gaussian random vector with $E[\mathbf{n}\mathbf{n}^H] = \sigma_n^2 I_{(M+1)N}$.

Assume the time delay of the $k$th user to be $\tau_k = (p_k + \delta_k)T_c$, where $p_k \in \{0, 1, \ldots, N-1\}$ is an integer and $\delta_k \in [0, 1)$ is the fractional part. The received signature waveform of the $i$th bit of the $k$th user, $\mathbf{d}_k(i) \in \mathcal{R}^{(M+1)N}$, can be expressed as the combination of two adjacent shifted versions of user spreading codes [7]

$$\mathbf{d}_k(i) = \delta_k \mathbf{c}_k(p_k + 1, i) + (1 - \delta_k) \mathbf{c}_k(p_k, i) \qquad (7)$$

where $\mathbf{c}_k \in \mathcal{R}^{(M+1)N}$ is the $k$th user's spreading code vector for the $(M+1)T$ second interval, defined as

$$\mathbf{c}_k = [c_k(0)\ c_k(1)\ \ldots\ c_k(N-1)\ \underbrace{0\ 0\ \ldots\ 0}_{MN}]^T. \qquad (8)$$

In (7), $\mathbf{c}_k(p_k, i)$ is defined as $\mathbf{c}_k$ right shifted by $(i-1)N + p_k$ chips. The chip-matched filtered and sampled signal of (3) can be expressed in more compact matrix form as

$$\mathbf{r} = \mathbf{DAb} + \mathbf{n} \qquad (9)$$

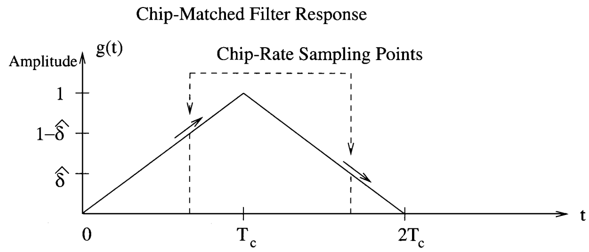


Fig. 1. Sampling of the chip-matched filter response for rectangular chip pulse shapes. Solid arrows represent the error in chip-matched filter response at the sampling points due to time-delay mismatch.

where $\mathbf{b} = [\mathbf{b}^T(1) \ \mathbf{b}^T(2) \ \ldots \ \mathbf{b}^T(M)]^T$, $\mathbf{b}(i) = [b_1(i) \ b_2(i) \ \ldots \ b_K(i)]^T$ is the data bit vector for the $i$th interval, $\mathbf{A} = \mathbf{I}_M \otimes \mathbf{a}$ is an $MK \times MK$ diagonal matrix of received signal amplitudes, where $\otimes$ denotes the Kronecker product, and $\mathbf{a} = \mathrm{diag}(a_1, a_2, \ldots, a_K)$. The code matrix is

$$\begin{aligned}\mathbf{D} = [&\mathbf{d}_1(1) \ldots \mathbf{d}_K(1) \, \mathbf{d}_1(2) \ldots \mathbf{d}_K(2) \ldots \\ &\mathbf{d}_1(M) \ldots \mathbf{d}_K(M)] \in \mathcal{R}^{(M+1)N \times MK} \end{aligned} \tag{10}$$

and the decorrelating detector with perfect time-delay information is constructed as [1]

$$\hat{\mathbf{b}} = \mathrm{sign}\,([\mathbf{D}^H\mathbf{D}]^{-1}\mathbf{D}^H\mathbf{r}). \tag{11}$$

## III. Robust Multiuser Detectors

### A. Prediction Error Approach

Denote the estimated time delay of the $k$th user as $\hat{\tau}_k = (p_k + \hat{\delta}_k)T_c$, where $p_k \in \{0, 1, \ldots, N-1\}$ and $\hat{\delta}_k \in [0, 1)$ is the fractional part. The $k$th user's signature waveform for the $i$th interval $\mathbf{d}_k(i)$ can be expressed as the weighted sum of two signals, as shown in Fig. 1.

$$\begin{aligned}\mathbf{d}_k(i) =& \delta_k \mathbf{c}_k(p_k+1, i) + (1-\delta_k)\mathbf{c}_k(p_k, i) \\ =& \left[\hat{\delta}_k \mathbf{c}_k(p_k+1, i) + (1-\hat{\delta}_k)\mathbf{c}_k(p_k, i)\right] \\ &+ (\delta_k - \hat{\delta}_k)\left[\mathbf{c}_k(p_k+1, i) - \mathbf{c}_k(p_k, i)\right] \\ \stackrel{\mathrm{def}}{=}& \hat{\mathbf{d}}_k(i) + (\delta_k - \hat{\delta}_k)\Delta\mathbf{d}_k(i). \end{aligned} \tag{12}$$

From (12), we can view each user as the combination of two virtual users, one with estimated code vector $\hat{\mathbf{d}}_k(i)$, and the other with error code vector $\Delta\mathbf{d}_k(i)$.

### B. Two-Virtual-User Approach

Similar to [16] and [17], these two virtual users can also be the chip-synchronous adjacent shifted versions of that user's spreading code signal, i.e.,

$$\begin{aligned}\mathbf{d}_k(i) =& \delta_k \mathbf{c}_k(p_k+1, i) + (1-\delta_k)\mathbf{c}_k(p_k, i) \\ \stackrel{\mathrm{def}}{=}& \delta_k \mathbf{d}'_{2k}(i) + (1-\delta_k)\mathbf{d}'_{2k-1}(i). \end{aligned} \tag{13}$$

### C. Hybrid Approach

Alternatively, rather than (12), the $k$th user's signature waveform for the $i$th interval $\mathbf{d}_k(i)$ can be expressed as a mixture between the previous two cases, i.e.,

$$\begin{aligned}\mathbf{d}_k(i) =& (1-\delta_k)\mathbf{c}_k(p_k, i) + \delta_k \mathbf{c}_k(p_k+1, i) \\ =& (1-\delta_k)\Big[(\hat{\delta}_k \mathbf{c}_k(p_k, i) + (1-\hat{\delta}_k)\mathbf{c}_k(p_k-1, i)) \\ &+ (1-\hat{\delta}_k)(\mathbf{c}_k(p_k, i) - \mathbf{c}_k(p_k-1, i))\Big] \\ &+ \delta_k \mathbf{c}_k(p_k+1, i) \\ \stackrel{\mathrm{def}}{=}& (1-\delta_k)\left[\hat{\mathbf{d}}_k(i) + (1-\hat{\delta}_k)\Delta\mathbf{d}_k(i)\right] \\ &+ \delta_k \mathbf{c}_k(p_k+1, i). \end{aligned} \tag{14}$$

Each user's code can now be viewed as the combination of three virtual users with code vectors $\hat{\mathbf{d}}_k(i)$, $\Delta\mathbf{d}_k(i)$, and $\mathbf{c}_k(p_k+1, i)$. We denote the vector $\mathbf{c}_k(p_k+1, i)$ of the third virtual user as the guard vector. The robust SIC detector based on (14) uses a similar technique as the prediction error approach.

The above decomposition has the advantage in that it contains the additional term $\mathbf{c}_k(p_k+1, i)$, which allows for fractional delay error correction across integer chip boundaries. Its disadvantage over (12) is noise enhancement when there is no integer chip error.

### D. Robust Decorrelating Detector

For simplicity, we consider the case of fractional delay uncertainty (Section III-A) only for the following algorithm description. In view of (12), the vector of received signal (9) is modified as

$$\mathbf{r} = \mathbf{D}'\mathbf{A}'\mathbf{b}' + \mathbf{n} \tag{15}$$

where $\mathbf{b}' = [\mathbf{b}^T(1) \ \mathbf{b}^T(2) \ \ldots \ \mathbf{b}^T(M) \ \mathbf{b}^T(1) \ \mathbf{b}^T(2) \ \ldots \ \mathbf{b}^T(M)]^T \in \mathcal{R}^{2MK}$, $\mathbf{A}' = \mathbf{I}_{2M} \otimes \mathbf{a}'$, $\mathbf{a}' = \mathrm{diag}(\,a_1, a_2, \ldots, a_K, (\delta_1 - \hat{\delta}_1)a_1, (\delta_2 - \hat{\delta}_2)a_2, \ldots, (\delta_K - \hat{\delta}_K)a_K\,)$, and code matrix

$$\begin{aligned}\mathbf{D}' =& [\hat{\mathbf{d}}_1(1) \ldots \hat{\mathbf{d}}_K(1) \, \hat{\mathbf{d}}_1(2) \ldots \hat{\mathbf{d}}_K(2) \ldots \hat{\mathbf{d}}_1(M) \ldots \\ &\hat{\mathbf{d}}_K(M) \, \Delta\mathbf{d}_1(1) \ldots \Delta\mathbf{d}_K(1) \, \Delta\mathbf{d}_1(2) \ldots \Delta\mathbf{d}_K(2) \\ &\ldots \Delta\mathbf{d}_1(M) \ldots \Delta\mathbf{d}_K(M)] \in \mathcal{R}^{(M+1)N \times 2MK}. \end{aligned} \tag{16}$$

We can now construct a robust decorrelating detector as

$$\hat{\mathbf{b}}' = \mathrm{sign}\,([\mathbf{D}'^H\mathbf{D}']^{-1}\mathbf{D}'^H\mathbf{r}). \tag{17}$$

Since the signal energy in the error vector may be small, we only use the signal energy in the estimated virtual user for bit detection, i.e.,

$$\hat{b}_k(i) = \hat{b}'_k(i), \qquad k = 1, \ldots, K, \text{ and } i = 1, \ldots, M. \tag{18}$$

Since (17) is a decorrelating detector, it does not depend on amplitude information and is near–far resistant under delay mismatch. However, since each user is decomposed into two virtual users, the total number of users that can be detected is upper bounded by $N/2$, where $N$ is the spreading factor [17]. The computational complexity of robust decorrelating detector is dominated by the doubled dimension matrix inversion, which is eight times that of the decorrelating detector.

### E. Multistage Robust Decorrelating Detector

One possible way to improve capacity and performance is to use a multistage version of the above robust decorrelating detector. At each stage, the $M$ error vectors of each user are combined into a long error vector based on the tentative data bit decisions, $\hat{b}_k(i)$, as

$$\mathbf{e}_k \stackrel{\text{def}}{=} \sum_{i=1}^{M} \Delta\mathbf{d}_k(i)\hat{b}_k(i), \qquad k = 1, \ldots, K. \tag{19}$$

We construct a new code matrix $\mathbf{D}''$, but with a smaller dimension than that of (16)

$$\mathbf{D}'' = [\hat{\mathbf{d}}_1(1)\ \ldots\ \hat{\mathbf{d}}_K(1)\ \hat{\mathbf{d}}_1(2)\ \ldots\ \hat{\mathbf{d}}_K(2)\ \ldots\ \hat{\mathbf{d}}_1(M)\ \ldots\ \hat{\mathbf{d}}_K(M)\ \mathbf{e}_1\ \ldots\ \mathbf{e}_K] \in \mathcal{R}^{(M+1)N \times (M+1)K}. \tag{20}$$

The multistage robust decorrelating detector is implemented by the following procedure.

Step 1) Use the standard decorrelating detector with estimated time delay to obtain the initial estimate

$$\hat{\mathbf{b}} = \text{sign}\left([\hat{\mathbf{D}}^H\hat{\mathbf{D}}]^{-1}\hat{\mathbf{D}}^H\mathbf{r}\right) \tag{21}$$

where $\hat{\mathbf{D}}$ is defined as in (10), but with $\hat{\mathbf{d}}_k(i)$ replacing $\mathbf{d}_k(i)$ for all $k$ and $i$.

Step 2) Construct code matrix $\mathbf{D}''$ using (19) and (20) based on the current tentative data bit decisions.

Step 3) Obtain tentative data bit decisions for the next stage via

$$\hat{\mathbf{b}}'' = \text{sign}([\mathbf{D}''^H\mathbf{D}'']^{-1}\mathbf{D}''^H\mathbf{r}). \tag{22}$$

Step 4) If the change of $\hat{\mathbf{b}}''$ from the previous stage is small enough, end the calculation. Otherwise, go to Step 2).

The number of users that can be supported is now $(M/M+1)N$. For moderate block lengths, such as $M = 9$, the capacity is now 90% of the spreading factor. Usually, the above multistage robust detector converges to a fixed point in three to four iterations. However, the inversion of a $(M+1)K \times (M+1)K$ matrix in (22) is still computationally complex.

### F. Robust SIC Detector

The decorrelating detector is the ML estimator when the user amplitude information is unknown at the receiver [1]. The linear SIC receiver is computationally attractive iterative implementation of the decorrelating detector with proven convergence properties [22], [23], which is similar to the space-alternating generalized expectation-maximization (SAGE) [24]-based iterative decorrelating detector [25]. Since a linear SIC implementation is used, reordering of the users according to signal-to-noise ratio (SNR) at each iteration is not necessary [23], and so is not performed here to reduce complexity.

We propose the following implementation of the above multistage robust decorrelating detector.

**Initialization:**
For $1 \le l \le K, 1 \le i \le M$, set:

$$\begin{aligned}
\Delta\mathbf{d}_l(i) &= \mathbf{c}_l(\hat{p}_l + 1, i) - \mathbf{c}_l(\hat{p}_l, i)\\
\hat{\mathbf{d}}_l(i) &= \hat{\delta}_l\mathbf{c}_l(\hat{p}_l + 1, i) + (1 - \hat{\delta}_l)\mathbf{c}_l(\hat{p}_l, i)\\
\hat{\mathbf{d}}_{l-dec}(i) &= [\hat{\mathbf{d}}_l(i)\ \Delta\mathbf{d}_l(i)]\ ([\hat{\mathbf{d}}_l(i)\ \Delta\mathbf{d}_l(i)]^H\\
&\quad [\hat{\mathbf{d}}_l(i)\ \Delta\mathbf{d}_l(i)])^{-1}\ [1\ 0]^H\\
\hat{a}_l^0(i) &= 0\\
\hat{b}_l^0(i) &= 0\\
\widehat{\Delta a}_l^{\,0} &= 0
\end{aligned}$$

**Iteration:**
For $j = 0, 1, \ldots$ do:
For $k = 1, 2, \ldots, K$ do:
Steps (1) through (4):
(1) Estimate user $k$'s received signal for the $(j + 1)$st iteration by subtracting other users' reconstructed signals and the residual signals from the received signal

$$\mathbf{r}_k^{j+1} = \mathbf{r} - \sum_{l=1}^{k-1}(\hat{\mathbf{r}}_l^{j+1} + \widehat{\Delta a}_l^{\,j+1}\mathbf{e}_l^{j+1}) - \sum_{l=k+1}^{K}(\hat{\mathbf{r}}_l^j + \widehat{\Delta a}_l^{\,j}\mathbf{e}_l^j) - \widehat{\Delta a}_k^{\,j}\mathbf{e}_k^j \tag{23}$$

where $\mathbf{e}_l^j = \sum_{i=1}^M \Delta\mathbf{d}_l(i)\hat{b}_l^j(i)$ and $\hat{\mathbf{r}}_l^j = \sum_{i=1}^M \hat{b}_l^j(i)\hat{a}_l^j(i)\hat{\mathbf{d}}_l(i)$ for $l \ge k$, and $\mathbf{e}_l^{j+1} = \sum_{i=1}^M \Delta\mathbf{d}_l(i)\hat{b}_l^{j+1}(i)$, $\hat{\mathbf{r}}_l^{j+1} = \sum_{i=1}^M \hat{b}_l^{j+1}(i)\hat{a}_l^{j+1}(i)\hat{\mathbf{d}}_l(i)$ and $\hat{b}_l^{j+1}(i) = \text{sign}\left((\hat{\mathbf{d}}_{l-dec}(i))^H\mathbf{r}_l^{j+1}\right)$ for $l < k$.
(2) Update user $k$'s signal amplitudes and data bits

$$\hat{a}_k^{j+1}(i) = \text{abs}\left((\hat{\mathbf{d}}_{k-dec}(i))^H\ \mathbf{r}_k^{j+1}\right) \tag{24}$$

$$\hat{b}_k^{j+1}(i) = \text{sign}\left((\hat{\mathbf{d}}_{k-dec}(i))^H\ \mathbf{r}_k^{j+1}\right) \tag{25}$$

where abs and sign take the absolute value and the sign, respectively.
(3) Estimate the residual signal of the $k$th user due to timing error as

$$\Delta\mathbf{r}_k^{j+1} = \mathbf{r}_k^{j+1} - \hat{\mathbf{r}}_k^{j+1} + \widehat{\Delta a}_k^{\,j}\mathbf{e}_k^j \tag{26}$$

(4) Update the amplitude of the error vector

$$\begin{aligned}
\mathbf{e}_k^{j+1} &= \sum_{i=1}^{M}\Delta\mathbf{d}_k(i)\hat{b}_k^{j+1}(i)\\
\widehat{\Delta a}_k^{\,j+1} &= \frac{1}{M}(\mathbf{e}_k^{j+1})^H(\Delta\mathbf{r}_k^{j+1}).
\end{aligned} \tag{27}$$

If for all $k = 1$ to $K$ and $i = 1$ to $M$, $|\hat{a}_k^{j+1}(i) - \hat{a}_k^j(i)|$ are below a threshold, end the calculation.

In the above algorithm, $([\hat{\mathbf{d}}_k(i)\ \Delta\mathbf{d}_k(i)]^H[\hat{\mathbf{d}}_k(i)\ \Delta\mathbf{d}_k(i)])^{-1}$ is used to decorrelate the signals in $\hat{\mathbf{d}}_k(i)$ and $\Delta\mathbf{d}_k(i)$, to prevent the self-interference from the residual signal due to timing error. When $\sigma_\tau < 0.2T_c$, the self-interference from the timing error residual signal is small, and it is advantageous to use $\hat{\mathbf{d}}_k(i)$ in place of $\hat{\mathbf{d}}_{k-dec}(i)$ in (24) and (25) to avoid the decorrelation-introduced noise enhancement. We note that since $\widehat{\Delta a}_k = \hat{a}_k(\delta_k - \hat{\delta}_k)$ from (12), $\widehat{\Delta a}_k$ can be used to improve the delay estimate. When there are large delay errors, we can always use $\hat{\mathbf{d}}_{k-dec}(i)$ in (24) and (25) first to bring the delay error within $0.2T_c$ and apply the robust SIC again using $\hat{\mathbf{d}}_k(i)$ for a second pass. Almost all current CDMA delay-estimation methods can provide delay error less than $0.2T_c$[6]–[10], so the first step is usually not needed, and thus, our analysis and simulation will largely be based on omitting self-interference decorrelation.

Our robust SIC adds an error vector signal estimation procedure to the original linear SIC. When the tentative data bit decisions at the $j$th iteration are all correct, then the estimated error vector signal will have an interference cancellation factor of 100%. When some bits of the tentative data bit decisions are incorrect, the estimated amplitude of the error vector will be smaller than the actual value, which is equivalent to soft cancellation with a factor less than 100%. So this robust SIC implicitly incorporates soft interference cancellation into its iterations, and will likely converge to the multistage robust decorrelating detector output. In the case when it does not converge to global maximum, good performance will still be expected. Strong users are more likely to have an accurate residual error signal estimate and cancellation. As a result, residual interference due to timing errors will be mostly cancelled out, and the local maximum will be close to the multistage robust decorrelating detector output.

In summary, the proposed robust SIC detector adds modest complexity to the standard SIC detector, but with interference caused by the timing errors dramatically reduced. Its capacity is close to that of the ideal decorrelating detector with the perfect time-delay estimates.

The above robust SIC detector can be extended to the multipath channels as well. Each resolvable signal path is divided into two virtual paths, and the delay error-introduced interference is estimated and cancelled for each path. The complexity increase from the single-path case is linearly proportional to the number of multipaths.

## IV. Performance Analysis

In this section, we will derive the the asymptotic multiuser efficiency (AME) and BER performance measure for the robust SIC detector. We also calculate the implementation complexity.

### A. AME and BER

The AME, a performance measure for multiuser signal detection as the background noise vanishes, for user $k$ is defined as [27]

$$\eta_k = \sup\left\{0 \le r \le 1 : \lim_{\sigma\to 0} \frac{P_k(\sigma)}{\mathcal{Q}\left(\frac{\sqrt{rw_k}}{\sigma}\right)} < +\infty\right\} \tag{28}$$

where $w_k$ is the received signal energy of user $k$, $\sigma$ is the standard deviation of white Gaussian noise, $P_k(\sigma)$ is the BER of user $k$ at the multiuser detector output, and $\mathcal{Q}(x) = \int_x^\infty (1/\sqrt{2\pi})e^{-y^2/2}dy$.

For the fractional chip uncertainty delay estimate case, the AME and BER of the proposed robust decorrelating detector are obtained similarly as the decorrelating detector [1]. The BER and AME for the $i$th bit of the $k$th user of the decorrelating detector with perfect time delay are, respectively

$$P_{k,i}(\sigma) = \mathcal{Q}\left(\frac{a_k}{\sigma\sqrt{(\mathbf{D}^H\mathbf{D})^{-1}_{(i-1)K+k}}}\right) \tag{29}$$

and

$$\begin{aligned}\eta_{k,i} =& max^2\left\{0, \frac{1}{\sqrt{(\mathbf{D}^H\mathbf{D})^{-1}_{(i-1)K+k}}}\right\}\\ =& \frac{1}{(\mathbf{D}^H\mathbf{D})^{-1}_{(i-1)K+k}}\end{aligned} \tag{30}$$

where $(\mathbf{D}^H\mathbf{D})^{-1}_{(i-1)K+k}$ denotes the $[(i-1)K+k, (i-1)K+k]$th element of the matrix $(\mathbf{D}^H\mathbf{D})^{-1}$.

For the robust decorrelating detector and the multistage decorrelating detector (assuming that tentative data bit decisions are all correct), the BER and AME are given as (29) and (30), with $\mathbf{D}'$ replacing $\mathbf{D}$.

In [21], it was shown that for a $K$-user CDMA system using independent and identically distributed (i.i.d.) random spreading sequences with spreading factor $N$, the average AME of a decorrelating detector is $\eta_K = (N - K/N - 1)$. Therefore, the AME is inversely proportional to the number of users. The robust decorrelating detector has an equivalent of $2K$ users. The multistage decorrelating detector described in Section III assuming correct tentative data bit decisions yield an equivalent of $(M + 1/M)K$ users. The robust SIC detector is an iterative implementation of the multistage decorrelating detector, so its performance would be upper bounded by the multistage decorrelator.

Note that in (24) we have estimated $\hat{a}_k(i)$ independently at different time intervals, $1 \le i \le M$, which converges to the decorrelating detector. If we use the constant amplitude property to average the $\hat{a}_k(i)$'s, i.e., $\hat{a}_k = (1/M)\sum_{i=1}^M \hat{a}_k(i)$, or use exact amplitude information (if it is available), then there will be less noise enhancement, and the robust SIC detector may outperform the corresponding decorrelating detector. However, convergence of such a smoothing procedure is not guaranteed.

The BER and AME for the $i$th bit of the $k$th user of the decorrelating detector with estimated time delays can be calculated as in [11]. As its AME depends on the received powers of the other users, it is not near–far resistant.

### B. Implementation Complexity

In this subsection, we calculate the computational complexity of the proposed robust SIC and compare it to those of the other multiuser detectors.

Note that in the decorrelation in the initialization step there are $MK$ $2\times 2$ matrices, each constructed from multiplying

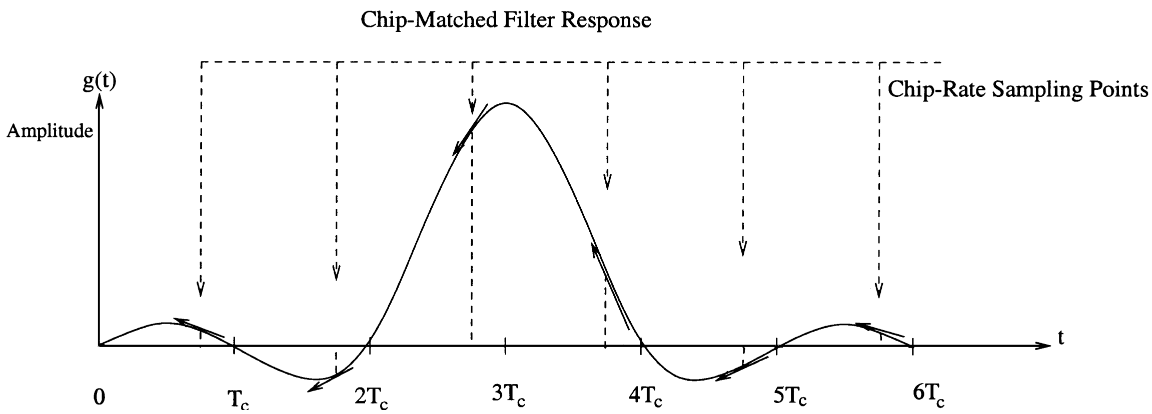


Fig. 2. Sampling of the chip-matched filter response for truncated bandlimited chip pulse shapes. The solid arrows represent the first-order derivative of the chip-matched filter response at the sampling points with estimated timing delay.

$2 \times N$ and $N \times 2$ matrices, and therefore is $O(MNK)$. Assume that the robust SIC needs $J$ iterations. Each iteration of the robust SIC algorithm takes $O(MNK)$ computations, so the total complexity is $O(JMNK)$. Usually $J = 10$ is enough to get close to steady-state performance. No reordering according to SNR is performed in the algorithm.

The decorrelating detector has complexity $O(M^3K^3)$. The SIC implementation of the decorrelating detector is of complexity $O(JMNK)$[23]. Assume that the number of SIC stages is the same as that of the robust SIC. The robust decorrelating detector [16], [17] has complexity $O(M^3K^3)$. The improved MMSE (IMMSE) multiuser detector [16], [26] has complexity at least $O(M^3K^3)$. Although the robust SIC doubles the complexity of that of SIC, its complexity is still far less than those of other robust multiuser detectors.

## V. Robust SIC Detector for Bandlimited Chip Pulse Shapes

Few research results have been reported on robust multiuser detectors with different chip pulse shapes. In [19], an approach similar to the IMMSE detector of [26] was extended to a pulse-shaping system, and a modified maximum-likelihood sequence detection (M-MLSD) is derived by averaging over the time-delay error distributions. In this section, we will construct a generalized system model for a bandlimited chip pulse shape CDMA system, and extend the proposed robust SIC detector of Section III to this general case.

The system model is similar to the one used in [19] and [22]. The received signal is given by (1), where the normalized signature waveform of user $k$ is modified from (2) as

$$\tilde{s}_k(t) = \sum_{j=0}^{N-1} c_k(j)\psi(t - jT_c) \tag{31}$$

where $\psi(t)$ is a bandlimited chip pulse shape. In the simulations, a square-root raised cosine pulse shape is used for $\psi(t)$. The receiver front end chip-matched filter has impulse response $\psi^*(t)$.

For general chip pulse shapes, the received signature waveform of the $i$th bit of the $k$th user, $\mathbf{d}_k(i)$, is the convolution of the user spreading codes with the chip-matched filter response at the sampling points, i.e.,

$$\mathbf{d}_k(i) = \mathbf{c}_k(p_k, i) * \mathbf{g}_k \tag{32}$$

where vector $\mathbf{g}_k$ is the $k$th user's chip-matched filter response at the chip-rate sampling points, as shown in Fig. 2. If the chip-matched filter response is truncated to length $PT_c$, then the vector $\mathbf{g}_k$ will be of length $P$, and the signature waveform $\mathbf{d}_k(i)$ will have $N + P - 1$ nonzero elements. The $m$th element of $\mathbf{g}_k$ is given by

$$g_k(m) = \int_{-\infty}^{\infty} \psi(\tau - \delta_k T_c)\psi^*(mT_c - \tau)d\tau, \quad m \in \{1, 2, \ldots, P\}. \tag{33}$$

The error vector $\Delta\mathbf{d}_k(i)$ for the bandlimited chip pulse shape is the convolution of the user spreading codes with the first derivative vector $\mathbf{f}_k$ of the $k$th user's chip-matched filter response at the sampling points, i.e.,

$$\Delta\mathbf{d}_k(i) = \mathbf{c}_k(p_k, i) * \mathbf{f}_k \tag{34}$$

with elements

$$f_k(m) = \frac{\partial}{\partial t}\int_{-\infty}^{\infty} \psi(\tau - \delta_k T_c)\psi^*(t - \tau)d\tau \mid_{t=mT_c}, \quad m \in \{1, 2, \ldots, P\}. \tag{35}$$

The $k$th user's waveform for the $i$th interval $\mathbf{d}_k(i)$ is first-order Taylor expanded as

$$\mathbf{d}_k(i) \approx \hat{\mathbf{d}}_k(i) + (\delta_k - \hat{\delta}_k)\Delta\mathbf{d}_k(i). \tag{36}$$

The robust SIC detector of Section III can be applied by substituting (34) and (36) into (12). Since the Taylor expansion of (36) is not exact, there will be residual interference. As will be shown in Section VI, this interference is not large as long as the timing error is small enough so that the first-order Taylor expansion is a good approximation.

## VI. Numerical and Simulation Results

In this section, we simulate the performance of our proposed robust SIC multiuser detector, and compare its performance to that of the decorrelating detector with and without perfect time-delay estimates.

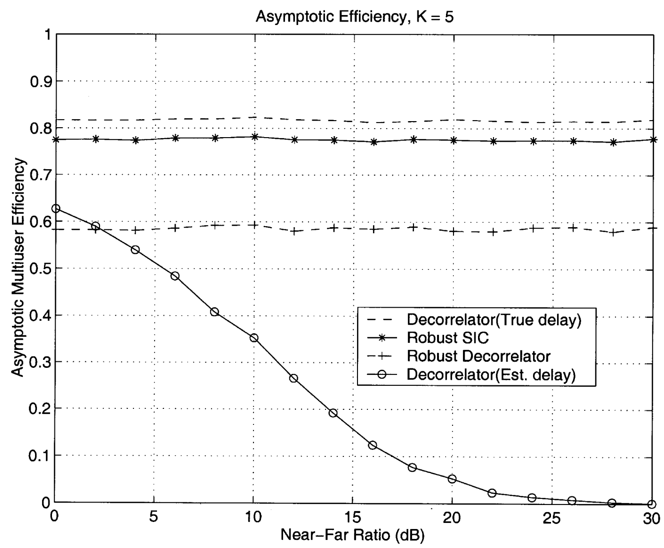


Fig. 3. AME as a function of near–far ratio for $\sigma_\tau = 0.1T_c$. $K = 5$ users.

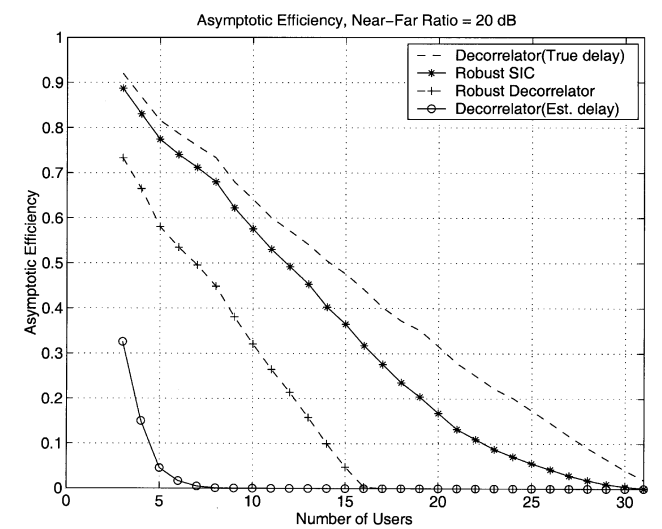


Fig. 4. AME as a function of number of users for $\sigma_\tau = 0.1T_c$. Near–far ratio is 20 dB.

Throughout the simulations, if it is not otherwise stated, we will assume, as in [11] and [29], that the delay estimation errors are independent zero-mean Gaussian random variables with equal standard deviation $\sigma_\tau = 0.1T_c$ for all users, and $\hat{\mathbf{d}}_k(i)$ is used rather than $\hat{\mathbf{d}}_{k-dec}(i)$ in (24) and (25). Gold code sequences of length $N = 31$ and a block size of $M = 9$ are used. Unless otherwise stated, the estimated time delays have only fractional chip uncertainty, and rectangular chip pulse shapes are used. Although a Gaussian delay-error distribution is used for the simulations, we note the robust SIC detector operation does not depend on the delay-error distribution. The user of interest, the first user, has the lowest received power. The near–far ratio is defined as the power ratio of the strongest user to the first user, $P_k/P_1$, where $P_k = a_k^2$. Other users have power levels uniformly distributed between the strongest and the weakest user. SNR is defined for the first user as $\mathrm{SNR} = P_1/\sigma_n^2$. For all the BER simulations, near–far ratio is fixed at 20 dB.

In Figs. 3–10, the *Decorrelator(True Delay)* curves refer to the decorrelating detector with true time delays, (11). *Decorrelator(Est. Delay)* refers to the decorrelating detector with estimated time delays, (21), *Robust SIC* refers to the robust SIC detector of (12) and (23)–(27), and *Robust Decorrelator* refers to the robust decorrelating detector with $2K$ virtual users of (17). As expected, the robust decorrelators employing virtual users as in (12) have almost identical BERs compared to that using (13). So in all the figures, only the curves of the robust decorrelator using (12) will be shown. The *Decorrelator(True Delay, Analytical)*, *Robust SIC(Analytical)*, and *Robust Decorrelator(Analytical)* curves refer to the analytical BER calculated using (29), with the SNR adjusted by a factor of 2/3, to account for the chip-asynchronous loss for rectangular chip pulses [28]. These analytical curves serve to confirm the accuracy of the BER simulation curves.

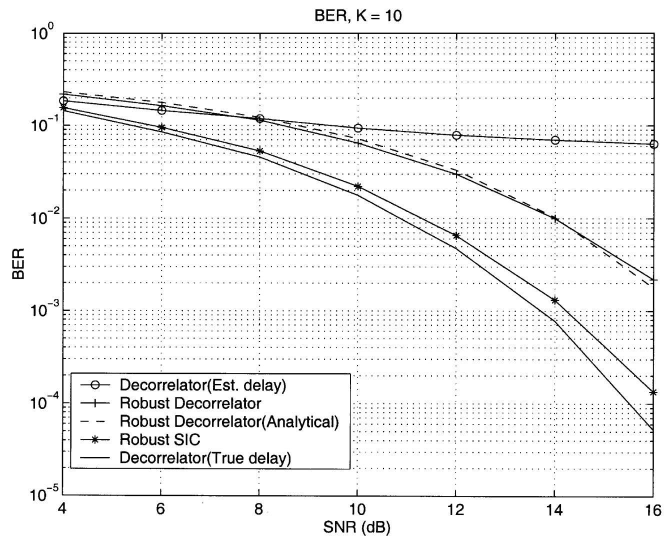


Fig. 5. BER of user 1 for $\sigma_\tau = 0.1T_c$. Proposed robust SIC detector with $K = 10$ users. Near–far ratio is 20 dB.

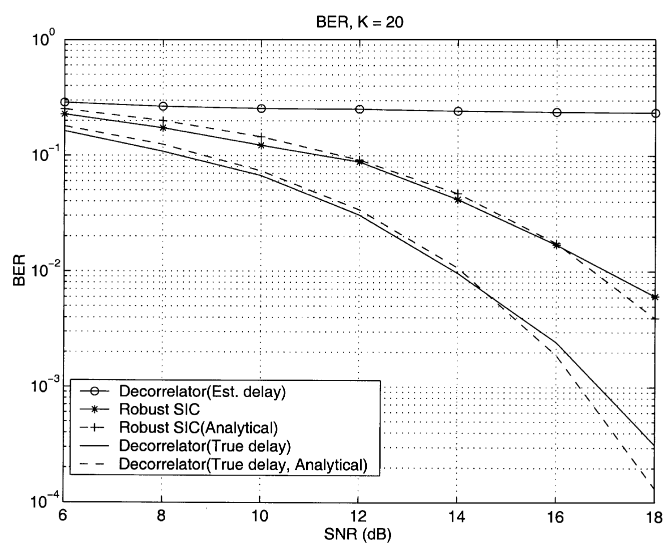


Fig. 6. BER of user 1 for $\sigma_\tau = 0.1T_c$. Proposed robust SIC detector with $K = 20$ users. Near–far ratio is 20 dB.

In Fig. 3, the number of users is $K = 5$ and the near–far ratio is increased from 0 to 30 dB. The multistage robust decorrelating detector with correct data bit decisions serves as the upper bound for the proposed robust SIC detector. As shown,

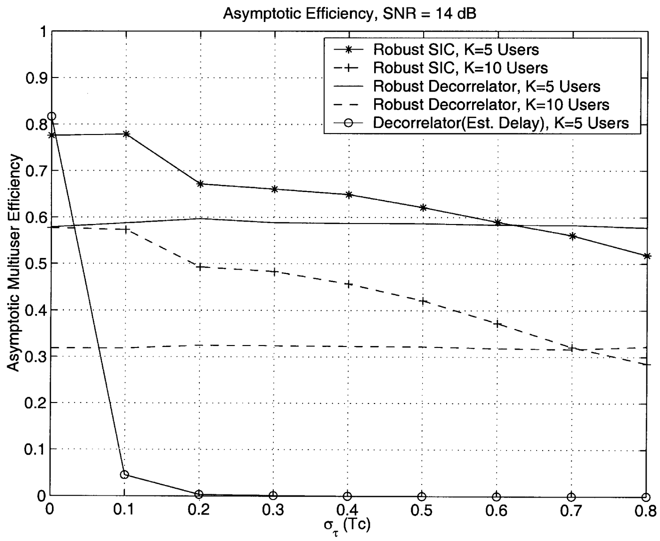


Fig. 7. AME of user 1 as a function of the delay error standard deviation $\sigma_\tau$. Near–far ratio is 20 dB.

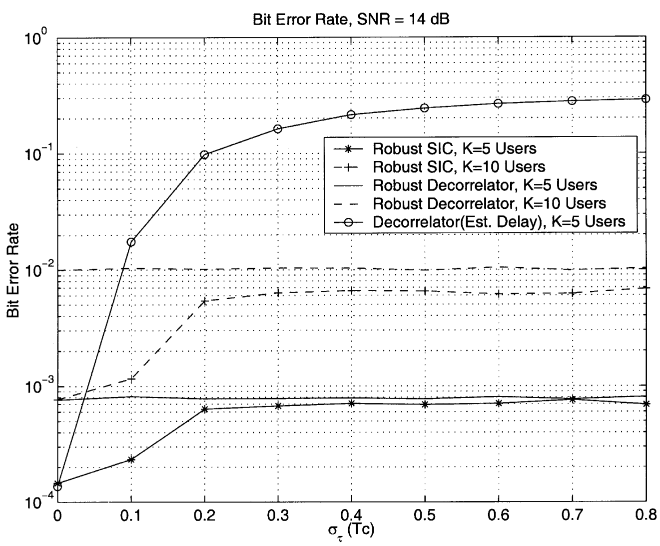


Fig. 8. BER of user 1 as a function of the delay error standard deviation $\sigma_\tau$. Near–far ratio is 20 dB.

the AME of the proposed robust SIC detector is between the AME value of the decorrelating detector with true delays and the robust decorrelating detector, and stays constant as the near–far ratio increases. Therefore, this proposed robust SIC detector exhibits near–far resistance under delay mismatch. As the near–far ratio increases, the AME of the decorrelating detector with estimated time delays decreases toward zero.

Fig. 4 compares the AME performance as the number of users is increased from 3 to 31. The near–far ratio is fixed at 20 dB. As expected from Section IV-A, the robust SIC can support $(M/M+1)N = 9/10 \times 31 \simeq 28$ users (AME is greater than zero). The decorrelator with estimated delays can only support five or six users, while the robust decorrelator can support 16 users, about half the spreading factor, $N/2$. It can also be observed that the AME of the robust decorrelator approaches zero at twice the rate of the decorrelator with true delays as the number of users increases, while the robust SIC decrease is close to that of the decorrelator with true delays.

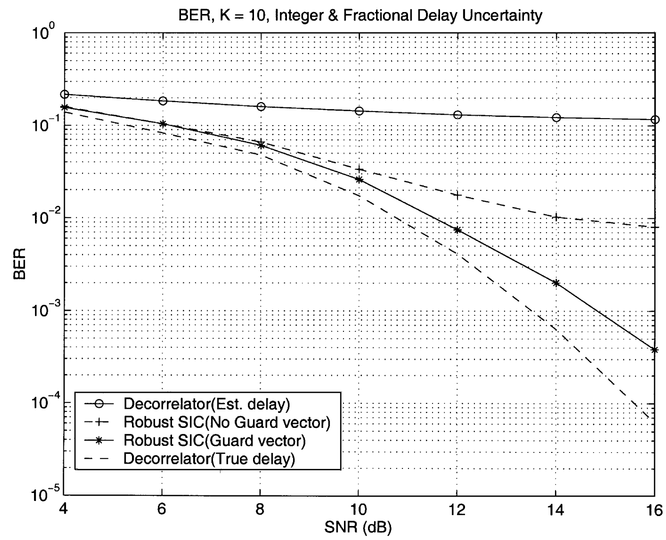


Fig. 9. Integer and fractional uncertainty delay estimates. BER of user 1 for $\sigma_\tau = 0.15T_c$ and $K = 10$ users. Near–far ratio is 20 dB.

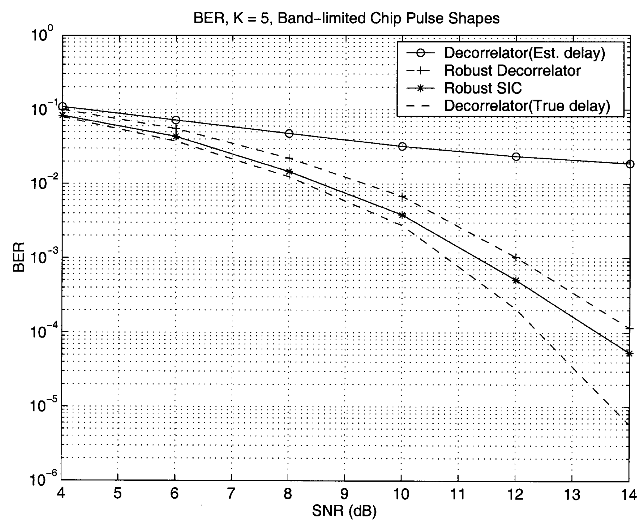


Fig. 10. Bandlimited chip pulse shapes. BER of user 1 for $\sigma_\tau = 0.1T_c$ and $K = 5$ users. Near–far ratio is 20 dB.

In Fig. 5, the results show that with ten users, the BER of the robust SIC detector (Section III-A) is lower than that of the robust decorrelator, and is close to the BER of the ideal decorrelator with known time delays. At a BER of $10^{-3}$, the loss compared to the ideal decorrelator is about 0.4 dB. The BER of the decorrelator with estimated delays is larger than $10^{-2}$ in high SNR, which makes it completely unusable in this severe near–far condition. We find that the proposed robust SIC detector converges in ten iterations, where we define convergence of the robust SIC detector to occur when the difference in estimated amplitude value between two consecutive iterations is less than 0.1%. As a result, the computational saving due to the SIC is large, compared to that of matrix inversion.

We have claimed that the robust SIC detector has a capacity of over 50% of the spreading factor. To show this, a system with 20 users is simulated in Fig. 6. The difference between the robust SIC detector and the decorrelator with true delays is significant. This can be explained by the AME values of Fig. 4, in which the AME of the robust SIC detector is about half of that of the ideal decorrelator.

Figs. 7 and 8 show the AME and BER of the proposed robust SIC, respectively, as a function of the values of delay estimation error standard deviation $\sigma_\tau$, varying from $0.0T_c$ to $0.8T_c$. The delay error is truncated to be within $\pm 0.5T_c$ as all users are assumed under acquisition. When $\sigma_\tau \geq 0.2T_c$, $\hat{\mathbf{d}}_{k-dec}(i)$ is used in (24) and (25). From the results, our robust SIC is usable as long as the estimated time delay is within $\pm 0.5T_c$ of the true delay, although its performance is best when $\sigma_\tau \leq 0.1T_c$.

In Fig. 9, performance of the two proposed approaches are compared for $\sigma_\tau = 0.15T_c$. *Robust SIC(Guard Vector)* refers to the robust SIC detector using (14) of Section III-C, and *Robust SIC(No Guard Vector)* refers to the robust SIC detector using (12) of Section III-A. From Fig. 9, as SNR gets larger, the robust SIC detector(Guard Vector) of (14) outperforms the robust SIC detector(No Guard Vector) of (12), as expected, since there is little noise enhancement, but at a cost of reduced capacity to $(M/M+2)N$.

Fig. 10 shows simulation results of the robust SIC detector for bandlimited chip pulse shapes with $K = 5$ users and the $\mathrm{SNR} = a_1^2 \int_{-\infty}^{\infty} \psi(t)^2 dt / \sigma^2 T_c$. From Fig. 10, the robust SIC detector has a lower BER than the robust decorrelating detector. Although both the BERs of the robust SIC detector and the robust decorrelating detector show significant improvement over the decorrelating detector with estimated delays, there is a larger performance gap from the ideal decorrelator, due to residual error in the first-order Taylor expansion in (36).

## VII. Conclusion

Using a chip-matched filtering model, we have proposed a robust SIC detector. The BER and AME performance measures are derived and simulated. The receiver is near–far resistant when all users are under acquisition to within a half chip. Performance is only slightly inferior to a decorrelating detector with perfect delay estimates, but outperforms a decorrelating detector with estimated delays. Capacity is greater than the 50% capacity limit of the synchronous robust decorrelating detector, and the AME is improved as well. This robust SIC detector is similar to iterative maximization of the log-likelihood function using the SAGE algorithm, which has guaranteed convergence, at least to a fixed point. This robust SIC detector, generalized to bandlimited chip pulse shapes, exhibits some performance degradation due to incomplete interference cancellation. This robust SIC detector is derived for AWGN or slowly varying channels. As further work, the approach could be extended to fast fading channels. In addition, receiver performance for bandlimited chip pulse shapes has room for further improvement.

## References


[1] R. Lupas and S. Verdú, "Near–far resistance of multiuser detectors in asynchronous channels," *IEEE Trans. Commun.*, vol. 38, pp. 496–508, Apr. 1990.

[2] U. Madhow and M. L. Honig, "MMSE interference suppression for direct-sequence spread-spectrum CDMA," *IEEE Trans. Commun.*, vol. 42, pp. 3178–3188, Dec. 1994.

[3] P. Patel and J. M. Holtzman, "Analysis of a simple successive interference cancellation scheme in a DS-CDMA system," *IEEE J. Select. Areas Commun.*, vol. 12, pp. 796–807, June 1994.

[4] M. K. Varanasi and B. Aazhang, "Multisatge detection in asynchronous code-division multiple-access communications," *IEEE Trans. Commun.*, vol. 38, pp. 509–519, Apr. 1990.

[5] J. Shen and Z. Ding, "Edge decision-assisted decorrelators for asynchronous CDMA channels," *IEEE Trans. Commun.*, vol. 47, pp. 438–445, Mar. 1999.

[6] R. L. Pickholtz, D. L. Schilling, and L. B. Milstein, "Theory of spread-spectrum communications – A tutorial," *IEEE Trans. Commun.*, vol. COM–30, pp. 855–884, May 1982.

[7] E. G. Ström, S. Parkvall, S. L. Miller, and B. E. Ottersten, "Propagation delay estimation in asynchronous direct-sequence code-division multiple-access systems," *IEEE Trans. Commun.*, vol. 44, pp. 84–93, Jan. 1996.

[8] S. E. Bensley and B. Aazhang, "Subspace-based channel estimation for code-division multiple-access communication systems," *IEEE Trans. Commun.*, vol. 44, pp. 1009–1020, Aug. 1996.

[9] ——, "Maximum-likelihood synchronization of a single user for code-division multiple-access communication systems," *IEEE Trans. Commun.*, vol. 46, pp. 392–399, Mar. 1998.

[10] D. Zheng, J. Li, S. L. Miller, and E. G. Ström, "An efficient code-timing estimator for DS-CDMA signals," *IEEE Trans. Signal Processing*, vol. 45, pp. 82–89, Jan. 1997.

[11] S. Parkvall, E. Ström, and B. Ottersten, "The impact of timing errors on the performance of linear DS-CDMA receivers," *IEEE J. Select. Areas Commun.*, vol. 14, pp. 1660–1668, Oct. 1996.

[12] F. Zheng and S. K. Barton, "On the performance of near–far resistant CDMA detectors in the presence of synchronization errors," *IEEE Trans. Commun.*, vol. 43, pp. 3037–3045, Dec. 1995.

[13] S. D. Gray, M. Kocic, and D. Brady, "Multiuser detection in mismatched multiple-access channels," *IEEE Trans. Commun.*, vol. 43, pp. 3080–3089, Dec. 1995.

[14] R. M. Buehrer, A. Kaul, S. Striglis, and B. D. Woerner, "Analysis of DS-CDMA parallel interference cancellation with phase and timing errors," *IEEE J. Select. Areas Commun.*, vol. 14, pp. 1522–1534, Oct. 1996.

[15] F. Cheng and J. M. Holtzman, "Effect of tracking error on DS/CDMA successive interference cancellation," in *Proc. IEEE Communication Theory Mini-Conf. (GLOBECOM )*, 1994, pp. 166–170.

[16] R. A. Iltis, "Domodulation and code acquisition using decorrelator detectors for QS-CDMA," *IEEE Trans. Commun.*, vol. 44, pp. 1553–1560, Nov. 1996.

[17] F. van Heeswyk, D. D. Falconer, and A. U. H. Sheikh, "A delay independent decorrelating detector for quasi-synchronous CDMA," *IEEE J. Select. Areas Commun.*, vol. 14, pp. 1619–1626, Oct. 1996.

[18] T. Östman, M. Kristensson, and B. Ottersten, "Asynchronous DS-CDMA detectors robust to timing errors," in *Proc. IEEE Vehicular Technology Conf.*, Jan. 1997, pp. 1704–1708.

[19] L. Chu and U. Mitra, "Approximate maximum-likelihood sequence detection for DS/CDMA systems with tracking errors," in *33rd Annu. Conf. Information Science and Systems*, Baltimore, MD, Mar. 1999, pp. 638–643.

[20] F. Zheng and S. K. Barton, "Near–far resistant detection of CDMA signals via isolation bit insertion," *IEEE Trans. Commun.*, vol. 43, pp. 1313–1317, Apr. 1995.

[21] R. R. Müller, P. Schramm, and J. B. Huber, "Spectral efficiency of CDMA systems with linear interference suppression," in *Proc. IEEE Workshop Kommunikationstechnik*, Jan. 1997, pp. 93–97.

[22] X. Wang and H. V. Poor, "Space–time multiuser detection in multipath CDMA channels," *IEEE Trans. Signal Processing*, vol. 47, pp. 2356–2374, Sept. 1999.

[23] L. K. Rasmussen, T. J. Lim, and A. Johansson, "A matrix-algebraic approach to successive interference cancellation in CDMA," *IEEE Trans. Commun.*, vol. 48, pp. 145–151, Jan. 2000.

[24] J. A. Fessler and A. O. Hero, "Space-alternating generalized expectation-maximization algorithm," *IEEE Trans. Signal Processing*, vol. 42, pp. 2664–2677, Oct. 1994.

[25] R. Wang and S. D. Blostein, "A spatial-temporal decorrelating receiver for CDMA systems with base-station antenna arrays," *IEEE Trans. Commun.*, vol. 49, pp. 329–340, Feb. 2001.

[26] L. Chu and U. Mitra, "Performance analysis of an improved MMSE multiuser receiver for mismatched delay channels," *IEEE Trans. Commun.*, vol. 46, pp. 1369–1380, Oct. 1998.

[27] S. Verdú, "Minimum probability of error for asynchronous Gaussian multiple-access channels," *IEEE Trans. Inform. Theory*, vol. IT–32, pp. 85–96, Jan. 1986.

[28] U. Madhow, "Blind adaptive interference suppression for direct-sequence CDMA," *Proc. IEEE*, vol. 86, pp. 2049–2069, Oct. 1998.

[29] L. Chu and U. Mitra, "Analysis of MUSIC-based delay estimators for DS-CDMA systems," *IEEE Trans. Commun.*, vol. 47, pp. 133–138, Jan. 1999.

**Wei Zha** (S'01) received the B.S. and M.S. degrees from Shanghai Jiao Tong University, Shanghai, China, in 1992 and 1995, respectively, both in electronics engineering. Since 1998, he has been working towards the Ph.D. degree and serving as a Research Assistant in the Department of Electrical and Computer Engineering, Queen's University, Kingston, ON, Canada.

He was a Lecturer and Research Engineer in the Department of Electronics Engineering, Shanghai Jiao Tong University, Shanghai, China, from 1995 to 1998. His research areas are in CDMA, OFDM, MIMO systems, and general areas of wireless communications and signal processing.

**Steven D. Blostein** (S'83–M'88–SM'96) received the B.S. degree in electrical engineering from Cornell University, Ithaca, NY, in 1983, and the M.S. and Ph.D. degrees in electrical and computer engineering from the University of Illinois, Urbana-Champaign, in 1985 and 1988, respectively.

He has been on the Faculty at Queen's University, Kingston, ON, Canada, since 1988, and currently holds the positions of Professor and Associate Head, Graduate Studies and Research in the Department of Electrical and Computer Engineering. He has been a consultant to both industry and government in the areas of document image compression, motion estimation, and target tracking, and was a Visiting Associate Professor in the Department of Electrical Engineering at McGill University, Montreal, QC, Canada, in 1995. He currently leads the Multirate Wireless Data Access Major Project sponsored by the Canadian Institute for Telecommunications Research. His current interests lie in statistical signal processing, wireless communications, and smart antennas.

Dr. Blostein served as Chair of IEEE, Kingston Section in 1993–1994, and as Associate Editor for the IEEE TRANSACTIONS ON IMAGE PROCESSING from 1996–2000. He is a registered Professional Engineer in Ontario, Canada.